Geometric thermodynamic uncertainty relation in a periodically driven thermoelectric heat engine

Jincheng Lu,[1,*] Zi Wang,[1,*] Jiebin Peng,[1] Chen Wang,[2,†] Jian-Hua Jiang,[3,‡] and Jie Ren[1,§]

[1]*Center for Phononics and Thermal Energy Science, China-EU Joint Laboratory on Nanophononics, Shanghai Key Laboratory of Special Artificial Microstructure Materials and Technology, School of Physics Science and Engineering, Tongji University, Shanghai 200092, China*

[2]*Department of Physics, Zhejiang Normal University, Jinhua, Zhejiang 321004, China*

[3]*Institute of Theoretical and Applied Physics, School of Physical Science and Technology & Collaborative Innovation Center of Suzhou Nano Science and Technology, Soochow University, Suzhou 215006, China*

(Received 8 January 2022; accepted 16 March 2022; published 25 March 2022)

The thermodynamic uncertainty relation, quantifying a trade-off among average current, the associated fluctuation (precision), and entropy production (cost), has been formulated at nonequilibrium steady state in various stochastic systems. Herein, we study the thermodynamic uncertainty relation in generic thermoelectric heat engines under periodic control protocols, by uncovering the underlying Berry-phase-like contribution. We show that our thermodynamic uncertainty relation breaks the seminal steady-state results, originating from the nonvanishing geometric effect. Furthermore, by deriving the consequent trade-off relation binding efficiency, power, and constancy, we prove that the periodically driven thermoelectric heat engines can generally outperform the steady-state analogies. The general bounds are illustrated by an analytically solvable two-terminal single quantum dot heat engine under the periodic modulation. Our work provides a geometric framework in bounding and optimizing a wide range of periodically driven thermoelectric thermal machines.

DOI: 10.1103/PhysRevB.105.115428

I. INTRODUCTION

Periodically driven quantum machines reach limited-cycle states after a long-time evolution since the coupling to the environment prevents infinite heating up [1–5]. These limited-cycle states form the basis of various functional thermal machines, which exhibit non-negligible fluctuations [6–8]. Investigating their trade-off relations provides insight into the optimal design principles for such periodically driven systems.

Recently, a thermodynamic uncertainty relation (TUR) has been formulated based on classical Markovian steady states, which demonstrates the trade-off relation between relative current fluctuation and dissipation [9–23]. Specifically, the average accumulated current $\langle Q\rangle$, its variance $\langle\langle Q^2\rangle\rangle \equiv \langle (Q-\langle Q\rangle)^2\rangle$, and the net entropy production $\langle\Sigma\rangle$ are universally bounded as

$$\frac{\langle\langle Q^2\rangle\rangle}{\langle Q\rangle^2}\langle\Sigma\rangle \geqslant 2. \tag{1}$$

It is known that the TUR was initially proposed in the long-time limit [9,24] and later generalized to the finite-time dynamics [25]. Consequently, the analysis methods and corresponding physical implications are further refined [26–28]. Although TUR has been widely applied in a tremendous amount of systems, it is not always valid. TUR violation corresponds to the situation that the left-hand side of Eq. (1) is smaller than 2. Quantum coherence [29], temporal driving [30–32], or magnetic field breaking time-reversal symmetry [26,33] may violate the original TUR.

For periodically driven systems, inferring the entropy production or at least an upper bound is generally more complex [31,32,34–41]. An early counterexample showed that a naive extension of the TUR from steady-state systems to periodically driven counterparts is inaccessible, since driving itself provides a spontaneous timescale enhancing current precision without significantly increasing the entropy production [42]. Subsequent attempts to find the analogy for periodically driven systems yield Proesman and van den Broeck's bound, which is valid for the time-symmetric driving [30]. Also, a series of general TURs incorporating the driving speed's effect are proposed both in discrete and continuous state spaces [31,32,43].

From the geometric view, the temporal modulation in phase space has an intrinsic effect on periodically driven transports and time-dependent energy conversion processes. Specifically, the geometric concepts are used in transient thermodynamics [44–48], in which the thermodynamic length [49] bounds the engine power and efficiency. The Berry-phase-like effect provides a nontrivial geometric contribution [50–62] to pump electric and heat currents against the thermodynamic bias. However, the intrinsic effects of the geometric phase on TUR and the performance of thermal machines are largely overlooked in previous studies. To address the geometric effect in time-dependent systems, in this work we study the TUR, heat-to-work conversion, and trade-off relation among energy efficiency, electric work, and work fluctuations in the periodically driven thermoelectric heat engines. In

*These authors contributed equally to this work.
†Corresponding author: wangchenyifang@gmail.com
‡Corresponding author: jianhuajiang@suda.edu.cn
§Corresponding author: xonics@tongji.edu.cn

 ©2022 American Physical Society

particular, we find that the nonvanishing geometric phase can simultaneously enhance the constancy of the engine and not significantly generate entropy production.

We highlight the difference between our work and previous studies here. First, our results are not restricted to time-symmetric driving protocols. In contrast, Ref. [30] breaks down in general asymmetric protocols. Second, we unveil the role of geometry in driven systems, which stays unclear in previously derived TUR relations [31,32,43]. Hence, the geometric phase may provide a versatile principle for implementing device design and optimization. Moreover, our framework could be readily generalized to more complex thermal machines possibly undertaking multitasks [63].

The paper is organized as follows. In Sec. II, we reorganize TUR by considering the intrinsic geometric origin and analyze the bounds on electric work and energy efficiency in periodically driven thermoelectric heat engines. We study the representative example and verify the validity of TUR via using a two-terminal single quantum dot system in Sec. III. We conclude in Sec. IV. Throughout this paper, we set the Boltzmann constant to the unit.

II. THE UNIVERSAL BOUNDS IN PERIODICALLY DRIVEN THERMOELECTRIC HEAT ENGINE

A. The general expression of the nonequilibrium current

Full counting statistics (FCS) [2] is considered as one powerful utility to characterize the nonequilibrium current and current fluctuations in a variety of fields, ranging from nonequilibrium transport, nonequilibrium statistics to quantum thermodynamics. FCS was initially proposed by Levitov *et al.* [64,65] to study the electron current statistics. Here, by including the counting field parameter λ, e.g., to count the particle and energy currents, the characteristic function after the long-time evolution $\mathcal{T}$ is expressed as [61,66]

$$\mathcal{Z}_\tau = \sum_{q=-\infty}^{+\infty} P_{\mathcal{T}}(q)e^{iq\lambda} = 1^\dagger \hat{T}\left[e^{\int_0^{\mathcal{T}} \mathcal{H}(\lambda,t)dt}\right]\mathbf{p}(0), \tag{2}$$

where $P_{\mathcal{T}}(q)$ is the probability distribution of the transferred quantity q during time $\mathcal{T}$. Here $1^\dagger = [1, 1]$, $\hat{T}$ denotes the time-ordering operator, and $\mathbf{p}(0) = [p_0(0), p_1(0)]^T$ are the initial occupation probabilities.

Then we present the expressions of the particle and heat currents for a general periodically driven system under the adiabatic modulation. According to the FCS and the adiabatic perturbation theory, the cumulant generating function is composed of two parts at the long-time ($\mathcal{T}$) limit [53,66]:

$$\begin{aligned} \mathcal{Z}_\tau &\approx e^{\mathcal{G}} = e^{(\mathcal{G}_{\rm dyn}+\mathcal{G}_{\rm geo})}, \\ \mathcal{G}_{\rm dyn} &= \int_0^{\mathcal{T}} dt\,\chi(\lambda,t), \\ \mathcal{G}_{\rm geo} &= -\int_0^{\mathcal{T}} dt\,\langle\varphi(\lambda)|\partial_t|\psi(\lambda)\rangle. \end{aligned} \tag{3}$$

Here χ denotes the eigenvalues of the evolution matrix $\mathcal{H}$ with the biggest real part. $|\psi(\lambda,t)\rangle$ and $\langle\varphi(\lambda,t)|$ are the corresponding normalized right and left eigenvector, respectively. Obviously, with a given parameter path it is generally found $\mathcal{G}_{\rm dyn} \propto 1/\Omega$, whereas $\mathcal{G}_{\rm geo}$ is independent of Ω. $\mathcal{G}_{\rm geo}$ is solely dependent on the geometric property of parameter spaces, rather than the specific parametrization (driving path) of protocols. Hence, it has a geometric nature.

The first component $\mathcal{G}_{\rm dyn}$ presents the temporal current average and contributes to the static particle and heat transport, while the second one, i.e., the geometric part $\mathcal{G}_{\rm geo}$, presents an additional contribution caused by the adiabatic cyclic evolution, and while requiring periodic modulation by two or more parameters. For the general case of periodically driven pairs $[u_1(t), u_2(t)]$, we have

$$\mathcal{G}_{\rm geo} = -\iint_{u_1u_2} du_1du_2\mathcal{F}_{u_1u_2}(\lambda), \tag{4}$$

$$\mathcal{F}_{u_1u_2} = \langle\partial_{u_1}\varphi|\partial_{u_2}\psi\rangle - \langle\partial_{u_2}\varphi|\partial_{u_1}\psi\rangle, \tag{5}$$

where $\mathcal{F}_{u_1u_2}$ is analogous with the gauge-invariant Berry curvature [67,68]. Finally we obtain the general expression of the nonequilibrium current accumulated during one period as

$$\langle J\rangle = \frac{\partial(\mathcal{G}_{\rm dyn}+\mathcal{G}_{\rm geo})}{\partial(i\lambda)}\Big|_{\lambda=0}, \tag{6}$$

and the fluctuation of the corresponding accumulated current is

$$\langle\langle J^2\rangle\rangle = \frac{\partial^2(\mathcal{G}_{\rm dyn}+\mathcal{G}_{\rm geo})}{\partial(i\lambda)^2}\Big|_{\lambda=0}. \tag{7}$$

B. The bound on fluctuations and entropy production

For periodically driven systems with a period $\mathcal{T} \equiv 2\pi/\Omega$ [31], Koyuk and Seifert derived a family of inequalities that relate entropy production with experimentally accessible data, including the mean, its dependence on driving frequency, and the variance of a large class of observables:

$$\frac{\langle\langle J^2(\Omega)\rangle\rangle}{\langle J(\Omega)\rangle^2}\langle\Sigma(\Omega)\rangle \geqslant 2\left[1-\Omega\frac{d\langle\bar{I}(\Omega)\rangle}{d\Omega}\frac{1}{\langle\bar{I}(\Omega)\rangle}\right]^2. \tag{8}$$

Here, $\bar{I} = J/\mathcal{T} \equiv \frac{1}{\mathcal{T}}\int_0^{\mathcal{T}} dtI(t)$ is the temporal average of the time-dependent current $I(t)$ along an *arbitrary* stochastic trajectory, J denotes the accumulated current of the periodically driven system, and $\langle\mathcal{O}\rangle$ is the ensemble average of a stochastic variable $\mathcal{O}$. The left-hand side of Eq. (8) involves the same expression of variables as the ordinary TUR does, where the dependence on Ω is exhibited, while the right-hand side additionally contains the derivative of the current with respect to the driving frequency, i.e., the response of the current to a slight change of the driving period. The above inequality is constructed in the large-$\mathcal{T}$ limit.

The current contribution is composed of two parts: the dynamical current and the geometric one, i.e., $\langle\bar{I}\rangle = \langle\bar{I}\rangle|_{\rm dyn} + \langle\bar{I}\rangle|_{\rm geo}$. The dynamical part is an average over the instantaneous steady state, whereas the geometric part originates directly from the change of such quasi-steady-state. In particular in the adiabatic regime, $\langle\bar{I}\rangle|_{\rm dyn}$ is independent of Ω, and the geometric current $\langle\bar{I}\rangle|_{\rm geo}$ is proportional to the driven frequency Ω [45,69]. The reason for this scaling will be explained in later sections. Consequently, the right-hand side of Eq. (8) can be simplified as $2/[1+\langle\bar{I}\rangle|_{\rm geo}/\langle\bar{I}\rangle|_{\rm dyn}]^2$. Thus, using the definition of accumulated current $J = \mathcal{T}\bar{I}$, we arrive

at the bound of TUR under periodic modulation:

$$\frac{\langle\langle J^2\rangle\rangle}{\langle J\rangle^2}\langle\Sigma\rangle \geqslant 2\left[\frac{1}{1+\langle J\rangle|_{\rm geo}/\langle J\rangle|_{\rm dyn}}\right]^2. \tag{9}$$

This is our first main result. For the case with finite thermodynamic bias, in the adiabatic limit $\Omega \to 0$ we general have the limit $\langle J\rangle|_{\rm geo}/\langle J\rangle|_{\rm dyn} \to 0$. The dynamical part of the current dominates the thermodynamic bound in Eq. (9). Accordingly, the thermodynamic bound reproduces the ordinary TUR [9]. However, one consequence of this relation is that it provides a generic condition for the (almost) dissipationless precision, while near the thermal equilibrium, the current becomes nearly proportional to the frequency of driving, where $\langle J\rangle|_{\rm geo} \gg \langle J\rangle|_{\rm dyn}$. The right-hand side vanishes. Therefore, temporally driven systems without the finite thermodynamic bias lie in the possible implementations, where this optimal limit may hold. It needs to be noted that this phenomenon is nonexistent at steady state.

C. The bound on electric work and energy efficiency in periodically driven thermoelectric heat engine

We consider a system isothermally coupled to several reservoirs with which it can exchange particles and energy. The total entropy production $\langle\Sigma\rangle$ under the stochastic thermodynamics [4] is specified by

$$T\langle\Sigma\rangle = -\langle W_{\rm out}\rangle + \langle W_d\rangle + \langle W_I\rangle. \tag{10}$$

On the right-hand side, the first term denotes the output work $\langle W_{\rm out}\rangle$ (useful work), the second term $\langle W_d\rangle$ represents dissipation (dissipated work), and the last term is the input energy $\langle W_I\rangle$ (done by the temporal driving) accumulated over one period. T is the temperature of the reservoirs. We restrict here to cyclic states, where the average entropy production of the middle system is zero in a full cyclic period. The positive energy current is defined from the reservoirs into the system.

In this subsection, we consider the heat engine regime ($\langle W_{\rm out}\rangle > 0$). We describe the traditional TUR bound as

$$\epsilon_p = \langle\Sigma\rangle\frac{\langle\langle W_{\rm out}^2\rangle\rangle}{\langle W_{\rm out}\rangle^2} \tag{11}$$

and the geometric TUR bound as

$$\epsilon_{\rm bound} = 2\left[\frac{1}{1+\langle W_{\rm out}\rangle|_{\rm geo}/\langle W_{\rm out}\rangle|_{\rm dyn}}\right]^2. \tag{12}$$

Then, based on the inequality in Eq. (9), we directly obtain the relation

$$\epsilon_p \geqslant \epsilon_{\rm bound}. \tag{13}$$

(i) When the input driving energy is positive, i.e., $\langle W_I\rangle > 0$, the free energy efficiency of the heat engine becomes [24]

$$\langle\eta\rangle \equiv \frac{\langle W_{\rm out}\rangle}{\langle W_d\rangle + \langle W_I\rangle} = \frac{\langle W_{\rm out}\rangle}{T\langle\Sigma\rangle + \langle W_{\rm out}\rangle}. \tag{14}$$

According to the above definition of efficiency $\langle\eta\rangle$, the relation Eq. (13) implies

$$\frac{1}{\langle\eta\rangle} \geqslant 1 + 2T\frac{\langle W_{\rm out}\rangle}{\langle\langle W_{\rm out}^2\rangle\rangle} \times\left[\frac{1}{1+\langle W_{\rm out}(\Omega)\rangle|_{\rm geo}/\langle W_{\rm out}(\Omega)\rangle|_{\rm dyn}}\right]^2 \equiv \frac{1}{\eta_{\rm bound}}, \tag{15}$$

when $\langle W_I\rangle > 0$.

(ii) When the driving energy is negative, i.e., $\langle W_I\rangle < 0$, the free energy efficiency of the heat engine is [70,71]

$$\langle\eta\rangle = \frac{\langle W_{\rm out}\rangle}{\langle W_d\rangle} = \frac{\langle W_{\rm out}\rangle}{T\langle\Sigma\rangle + \langle W_{\rm out}\rangle - \langle W_I\rangle}. \tag{16}$$

Combined with the relation Eq. (13), the efficiency $\langle\eta\rangle$ is bounded by

$$\frac{1}{\langle\eta\rangle} \geqslant 1 + 2T\frac{\langle W_{\rm out}\rangle}{\langle\langle W_{\rm out}^2\rangle\rangle} \times\left[\frac{1}{1+\langle W_{\rm out}(\Omega)\rangle|_{\rm geo}/\langle W_{\rm out}(\Omega)\rangle|_{\rm dyn}}\right]^2 - \frac{\langle W_I\rangle}{\langle W_{\rm out}\rangle|_{\rm dyn} + \langle W_{\rm out}\rangle|_{\rm geo}} \equiv \frac{1}{\eta_{\rm bound}}. \tag{17}$$

Equations (15) and (17) are our second main results. In general, the output work of a steady-state heat engine vanishes as its free energy efficiency approaches the unit [72–74]. A finite power at this limit in principle is possible only if the current fluctuations diverge [13] or if the output power is proportional to the driving frequency of the engine [31]. Although these general results have been preliminarily demonstrated in previous studies [31,32], our work provides a general realizable optimization principle. Specifically, by maximizing the geometric contribution $\langle W_{\rm out}\rangle|_{\rm geo}$ using geometric methods and minimizing the dynamical contribution $\langle W_{\rm out}\rangle|_{\rm dyn}$, we may push these bounds [Eqs. (15) and (17)] to a more efficient regime.

III. VERIFYING THE VALIDITY OF THE THERMODYNAMIC UNCERTAINTY RELATION IN PERIODICALLY DRIVEN THERMOELECTRIC HEAT ENGINE

A. Single-level quantum dot system

We illustrate the formal results within the two-terminal system. In our construction (see Fig. 1), a single quantum dot (QD) system exchanges energy with two electronic reservoirs, L and R, which can be set out of equilibrium with a finite voltage bias $\Delta\mu$ or/and temperature difference ΔT. Our model is described by the Hamiltonian

$$\hat{H} = \hat{H}_S + \hat{H}_B + \hat{H}_I, \tag{18}$$

where $\hat{H}_S = E_0 c_d^\dagger c_d$ denotes the single-level QD, $\hat{H}_B = \sum_{v=L,R}\sum_k \epsilon_{kv} c_{kv}^\dagger c_{kv}$ represents the left and right electronic reservoirs (source and drain), and $\hat{H}_I = \sum_{v=L,R}\sum_k t_{kv}(c_{kv}^\dagger c_d + \text{H.c.})$ is the system-reservoir interaction. The working substance consists of a single electronic level with the creation (annihilation) operator

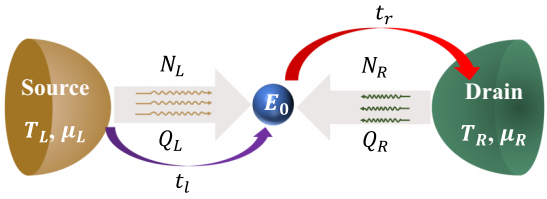

FIG. 1. Schematic of the single-level QD system. An electron from the source (with the chemical potential μ_L and the temperature T_L) flows across the QD with the energy E_0 and hops into the drain (with the chemical potential μ_R and the temperature T_R). The energy level E_0 in the QD and the coupling strengths t_i $(i = l, r)$ between the dot and the reservoir can generally be considered as time-dependent driving parameters.

$c_d^\dagger$ (c_d) and time-dependent energy $E_0(t)$. The dot is coupled to two fermionic reservoirs (leads) $v = L, R$, which may have different temperatures. $c_{kv}^\dagger$ (c_{kv}) creates (annihilates) an electron with energy ϵ_{kv} in the v lead that couples to the central level, with t_{kv} being the tunneling rate. The v lead is characterized as the Fermi-Dirac distribution function $f_v(\omega) = \{\exp[(\omega - \mu_v)/k_B T_v] + 1\}^{-1}$, with the temperature T_v and the chemical potential μ_v. The reservoirs exert dissipative effects on the dynamics, described by the spectral function $\Gamma_v(\epsilon) = 2\pi \sum_k t_{kv}^2 \delta(\epsilon - \epsilon_k)$.

Using the Redfield approximation for weak system-bath coupling [75–78], the dynamics of the QD can be modeled as

$$\dot{p}_0^\lambda(t) = -k_u\, p_0^\lambda(t) + k_d^\lambda\, p_1^\lambda(t), \tag{19a}$$

$$\dot{p}_1^\lambda(t) = k_u^\lambda\, p_0^\lambda(t) - k_d\, p_1^\lambda(t). \tag{19b}$$

Here λ is the counting parameter induced by quantum transitions, which can be used to calculate the fluctuation properties of an arbitrary current, e.g., heat and particle. These equations can be reexpressed in a matrix form as

$$\frac{d|p^\lambda(t)\rangle}{dt} = \mathcal{H}(\lambda)|p^\lambda(t)\rangle, \tag{20}$$

where $|p^\lambda(t)\rangle = (p_0^\lambda(t), p_1^\lambda(t))$. p_n $(n = 0, 1)$ denotes the probability of QD to occupy the state $|n\rangle$, satisfying $p_0(t) + p_1(t) = 1$ [79]. The excitation and relaxation rates with the counting field read

$$k_u^\lambda = k_{0\to1}^L + k_{0\to1}^R e^{i\lambda_p + iE_0\lambda_E}, \tag{21a}$$

$$k_d^\lambda = k_{1\to0}^L + k_{1\to0}^R e^{-i\lambda_p - iE_0\lambda_E}, \tag{21b}$$

where $k_{0\to1}^v = \Gamma_v f_v(E_0)$, $k_{1\to0}^v = \Gamma_v[1 - f_v(E_0)]$ [80–83], and λ_E and λ_p are the counting fields for energy and particles, respectively. Without loss of generality, here we count the flow between the system and the right reservoir. Here we define the positive current flowing from external reservoirs into the middle system.

Finally, the steady-state particle and energy currents flowing from the right reservoir into the system are expressed as [84,85]

$$\langle I_p^R\rangle_s = \frac{\Gamma_L\Gamma_R[f_R(E_0) - f_L(E_0)]}{\Gamma_L + \Gamma_R}, \tag{22a}$$

$$\langle I_E^R\rangle_s = \frac{E_0\Gamma_L\Gamma_R[f_R(E_0) - f_L(E_0)]}{\Gamma_L + \Gamma_R}, \tag{22b}$$

while $\langle I_Q\rangle$ is the net heat current carried by the electrons, $\langle I_Q^R\rangle = \langle I_E^R\rangle - \mu_R \langle I_p^R\rangle$. These steady-state results are of the typical Landauer type in thermal transports [76]. The flows from the left and right reservoirs are not independent. Particle conservation implies that $\langle I_p^L\rangle_s + \langle I_p^R\rangle_s = 0$, while energy conservation requires $\langle I_E^L\rangle_s + \langle I_E^R\rangle_s = 0$ [6,86].

B. Geometric Berry-phase-induced particle and energy currents

The single-QD system connected to two reservoirs is subjected to cyclic parameter modulations. This could be realized by imposing a modulation on either of the following parameters: $\Gamma_v(t)$, $\mu_v(t)$, $T_v(t)$ $(v = L, R)$, and $E_0(t)$ [87,88]. Here, we count the particle and energy currents from the right (R) reservoir into the single-QD system. Based on the general expression of the current in Eq. (6), the accumulated particle current flowing by including the parameters λ_p and λ_E are obtained as

$$\langle N_R\rangle = \frac{\partial(\mathcal{G}_{\rm dyn} + \mathcal{G}_{\rm geo})}{\partial(i\lambda_p)}\Big|_{\lambda_p=0} \tag{23}$$

and

$$\langle E_R\rangle = \frac{\partial(\mathcal{G}_{\rm dyn} + \mathcal{G}_{\rm geo})}{\partial(i\lambda_E)}\Big|_{\lambda_E=0}, \tag{24}$$

respectively. And the electronic heat extracted from the right reservoir is defined as $Q_R(t) = E_R(t) - \mu_R N_R(t)$. Similarly, the particle current N_L and energy current E_L flowing from the left (L) reservoir into the central system can also be obtained by introducing the excitation and relaxation rates with the counting fields as $k_u^\lambda = k_{0\to1}^L e^{i\lambda_p + iE_0\lambda_E} + k_{0\to1}^R$, $k_d^\lambda = k_{1\to0}^L e^{-i\lambda_p - iE_0\lambda_E} + k_{1\to0}^R$. The fluctuation of the current is $\langle\langle (N_R)^2\rangle\rangle = \partial^2\mathcal{G}/\partial(i\lambda_p)^2|_{\lambda=0}$, where $\langle\langle N_R^2\rangle\rangle = \langle N_R^2\rangle - \langle N_R\rangle^2$ is the second cumulant. Other higher-order cumulants can be calculated accordingly. Considering the scaling of $\mathcal{G}_{\rm geo}$ and $\mathcal{G}_{\rm dyn}$ with respect to Ω, we have $\langle J\rangle|_{\rm geo} \propto 1$ and $\langle J\rangle|_{\rm dyn} \propto 1/\Omega$. Consequently, $\langle \bar{I}\rangle|_{\rm geo} \propto \Omega$ and $\langle \bar{I}\rangle|_{\rm dyn} \propto 1$. Here, Q is an arbitrary accumulated current and $\bar{I} \equiv Q/\mathcal{T}$ is the time-averaged current. It should be noted that these scaling properties validate the derivation of Eq. (9).

We restrict our discussed protocols around the period $\mathcal{T} = 10^{-11}$ s, which corresponds to $\hbar\Omega \approx 0.4$ meV. Comparing to $\hbar\Omega$, the dissipation strengths $\Gamma_L = 10$ meV and $\bar{\Gamma}_R = 20$ meV are much greater than $\hbar\Omega$. This allows our applying the adiabatic (small driving frequency) approximation in Eq. (3) to be valid. In this regime, $\mathcal{G}_{\rm geo}$, given in Eq. (4) and Eq. (5), only depends on the geometric properties in the parameter space, which is an intrinsic geometric quantity.

We now turn to the first law of thermodynamics for a time-dependent quantum thermal machine [85]. Specifically, the particle conversation is characterized as $N_L + N_R = \Delta n$ and the energy conversation is quantified by [61,71,89–91] $E_L + E_R + W_I = \Delta U$, where Δn and ΔU are the stochastic number and energy changes of the reduced quantum system, e.g., the QD, throughout the transition processes. The input power induced by the temporal driving provides a nontrivial term W_I. Since terms on the left-hand sides of conservation laws are growing with time and the right-hand sides are naturally bounded by the size of the reduced quantum system, we arrive at the approximate conservation laws at the long-time

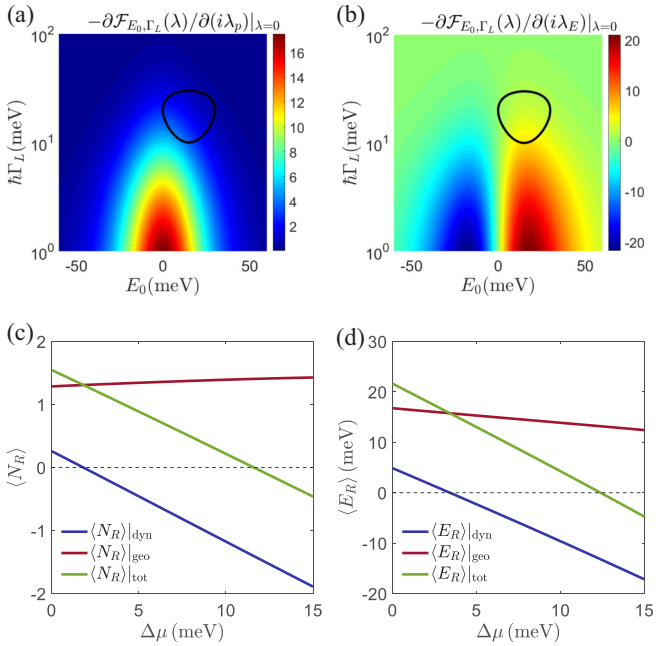

FIG. 2. The contour map in the parameter space of the dot energy level E_0 and the left reservoir's spectral function Γ_L: (a) Berry curvature for the average particle current $-\partial\mathcal{F}_{E_0\Gamma_L}(\lambda)/\partial(i\lambda_p)|_{\lambda=0}$ and (b) Berry curvature for the average energy current $-\partial\mathcal{F}_{E_0\Gamma_L}(\lambda)/\partial(i\lambda_E)|_{\lambda=0}$. (c) The particle current $\langle N_R\rangle$ and (d) the energy current $\langle E_R\rangle$ as a function of $\Delta\mu$. The other parameters are given by $\mu = 0$ (mean value), $\hbar\Gamma_R = 10$ meV, $k_BT_L = 10$ meV, and $k_BT_R = 1.2k_BT_L$. The energy modulations are exemplified as $E_0 = [15 + 15\sin(\Omega t)]$ meV, $\hbar\Gamma_L = [20 + 10\sin(\Omega t + \pi/2)]$ meV, $\Omega = 2\pi/\mathcal{T}$, and $\mathcal{T} = 10^{-11}$ s.

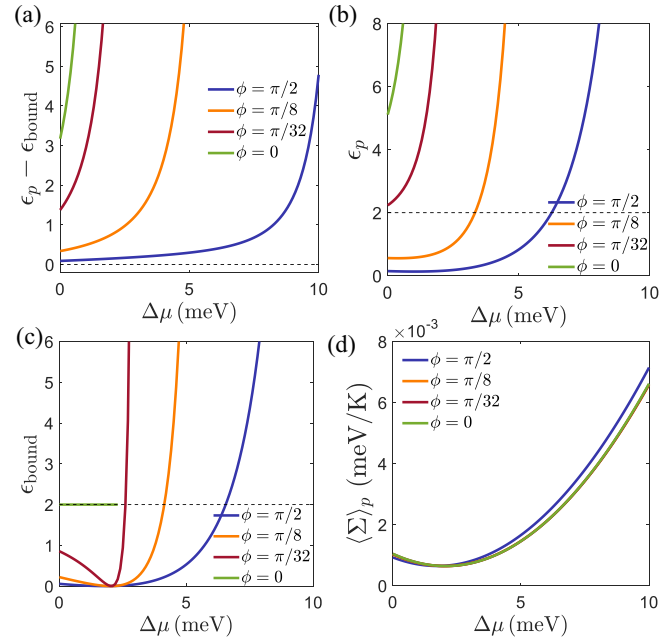

FIG. 3. (a) The distance of the traditional TUR bound ϵ_p (11) from the geometric TUR bound $\epsilon_{\rm bound}$ (12), (b) the traditional TUR bound ϵ_p, (c) the geometric TUR bound $\epsilon_{\rm bound}$, and (d) the average entropy production $\langle\Sigma\rangle_p$ as functions of $\Delta\mu$ for different phase ϕ. The parameters are $\mu = 0$, $\hbar\Gamma_R = 10$ meV, $k_BT_L = 10$ meV and $k_BT_R = 12$ meV, $E_0 = [15 + 15\sin(\Omega t + \phi)]$ meV, $\hbar\Gamma_L = [20 + 10\sin(\Omega t)]$ meV, $\Omega = 2\pi/\mathcal{T}$, and $\mathcal{T} = 10^{-11}$ s.

(large period number) limit [92,93]

$$\langle N_L\rangle + \langle N_R\rangle = 0,$$
$$\langle E_L\rangle + \langle E_R\rangle + \langle W_I\rangle = 0. \tag{25}$$

Here, $\langle N_v\rangle$ is the average accumulated input particle number into reservoir v, $\langle E_v\rangle$ is the input energy flowing from reservoir v, and $\langle W_I\rangle$ is the extra work done by driving. These stochastic quantities are accumulated during a long-time interval.

We further proceed by presenting simulation results at finite temperature and voltage bias, focusing on the large-bias limit rather than the linear-response behavior. For convenience, we define the chemical potential difference $\Delta\mu = \mu_L - \mu_R$ and the mean chemical potential $\mu \equiv (\mu_L + \mu_R)/2$. Then, we fix the mean chemical potential μ at zero and study the effect of $\Delta\mu$. To operate the device as a thermoelectric engine, we assume $T_L < T_R$ and $\Delta\mu > 0$. The produced electronic work after a period of driving cycle of the thermoelectric heat engine is given by [70,94]

$$\langle W_{\rm out}\rangle = -(\mu_R - \mu_L)\langle N_R\rangle. \tag{26}$$

In Fig. 2, we demonstrate the geometric thermoelectric pump effect. We illustrate that by modulating parameters, i.e., the system-reservoir coupling strength Γ_L and the QD energy level E_0, the nontrivial Berry curvatures in Figs. 2(a) and 2(b) yield both nonvanishing geometric particle and energy currents, as shown in Figs. 2(c) and 2(d). We note that our setup is within the reach of current experiment platforms [95–97]. Hence, the geometric currents currently could be experimentally detected [62].

As one main result, we show that the Berry-phase effect acts as a reconfigurable pump, providing additional particle and heat currents across the QD system with no static bias or even against the direction of biases. This exhibits the power of our framework. By tailoring the driving path in the parameter space, we can both design the functionality of thermoelectric engines and modulate the ratio of the geometric and the dynamic components of currents, and therefore optimize the engine's performance bounds proposed in Sec. II. We elaborate this point in the following sections.

C. Verifying the validity of the TUR relation

In Figs. 3 and 4, we verify the bounds on fluctuations and entropy production in periodically driven systems. We concentrate on the effect of geometric properties, which can be characterized by the relative phases ϕ. Different ϕ represents different driving protocols. Specifically, parameters are driven as $[u_1(\Omega t), u_2(\Omega t + \phi)]$, with $u_1(\Omega t)$ and $u_2(\Omega t)$ being in phase. $\phi = \pi/2$ is the situation where the geometric contribution is optimized. In contrast, if the phase $\phi = 0$, the geometric contribution vanishes and there is *only* the dynamical counterpart. This is obvious since the encircled area in the parameter space disappears, when $\phi = 0$.

In this work, we focus our discussions on the working regime of periodically driven thermoelectric heat engine, i.e.,

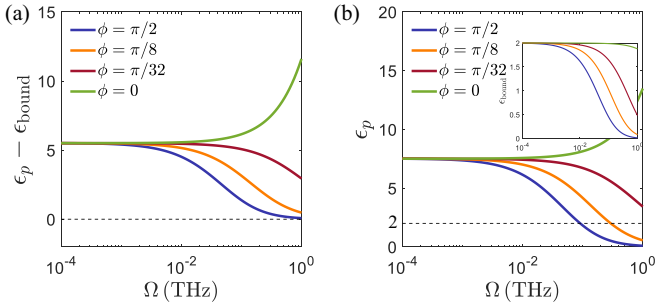

FIG. 4. (a) The distance of realized ϵ from the geometric TUR bound $\epsilon_{\rm bound}$ and (b) the original TUR bound ϵ_p, as functions of driving frequency Ω for different modulation phases. Inset: The geometric TUR bound $\epsilon_{\rm bound}$ as a function of driving frequency Ω. The parameters are $\Delta\mu = 1$ meV, $\mu = 0$, $\hbar\Gamma_R = 10$ meV, $k_BT_L = 10$ meV and $k_BT_R = 15$ meV, $E_0 = [15 + 15\sin(\Omega t + \phi)]$ meV, $\hbar\Gamma_L = [20 + 10\sin(\Omega t)]$ meV, and $\Omega = 2\pi/\mathcal{T}$.

$\langle W_{\rm out}\rangle > 0$. Here, $W_{\rm out}$ is the useful output work of the stochastic thermoelectric work. From Figs. 3(a) and 4(a), we find that regardless of phase ϕ, voltage bias $\Delta\mu$, and the driving frequency Ω, the proposed geometric TUR bound $\epsilon_{\rm bound}$ (12) is perfectly below the traditional TUR bound ϵ_p (11). The bounds on fluctuations and entropy production are always satisfied. Moreover, as shown in Fig. 3(b), if the geometric current vanishes, the TUR bound is reduced to the steady-state limit (1), which is exhibited in Fig. 3(c) with $\phi = 0$ and the inset of Fig. 4(b) with $\Omega \to 0$. This is consistent with steady-state transport for classical Markov processes [9,24].

As the modulation phase ϕ becomes finite, e.g., $\phi = \pi/8$ and $\phi = \pi/2$, the geometric component dominates the heat transport and fluctuations. As a consequence, the original TUR bound breaks down ($\epsilon_p < 2$), e.g., at the small voltage bias in Fig. 3(b). In sharp contrast, our geometric TUR bound is still robust ($\epsilon_{\rm bound} \geqslant 0$), as shown in Fig. 3(c). In particular, $\epsilon_{\rm bound}$ becomes vanishing as the voltage bias is around 3 meV, nearly regardless of the modulation phase ϕ. Generally, the geometric-phase-induced particle current $\langle N_R\rangle|_{\rm geo}$ is positive and finite, as exemplified in Fig. 2(c). However, the dynamical component $\langle N_R\rangle|_{\rm dyn}$ is reduced with an increase of $\Delta\mu$. Based on Eq. (22a), the corresponding vanishing position, termed the dynamic current cutoff voltage, can be obtained as $\langle N_R\rangle|_{\rm dyn} \approx 0$. This directly results in $\epsilon_{\rm bound} \approx 0$, for $\langle W_{\rm out}\rangle|_{\rm geo}/\langle W_{\rm out}\rangle|_{\rm dyn} \to \infty$. Moreover, if we further increase $\Delta\mu$ beyond the dynamic current cutoff voltage, it is found that $\langle N_R\rangle|_{\rm dyn}$ is negatively enhanced. Hence, the total current cutoff voltage can be obtained when $\langle N_R\rangle|_{\rm dyn} + \langle N_R\rangle|_{\rm geo} = 0$, which can be observed in Fig. 3(c) with divergent $\epsilon_{\rm bound}$ and Fig. 5(a) with zero output electric work.

Then we consider harvesting the energy from the (hot) reservoir for regulating the QD system to generate electricity. The entropy production of the whole system is described as $\langle\Sigma\rangle_p = -\sum_{v=L,R}\langle Q_v\rangle/T_v$ [98]. Including the energy and particle conversations [Eq. (25)], the entropy production is given by

$$T_L\langle\Sigma\rangle_p = -\langle W_{\rm out}\rangle + (1 - T_L/T_R)\langle Q_R\rangle + \langle W_I\rangle, \tag{27}$$

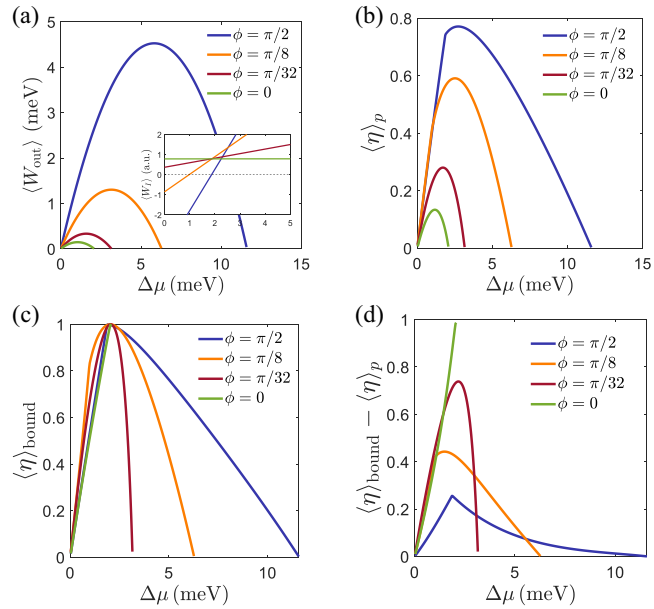

FIG. 5. (a) The output electric work $\langle W_{\rm out}\rangle$, (b) the energy efficiency $\langle\eta\rangle_p$, (c) $\langle\eta\rangle_{\rm bound}$, and (d) $\langle\eta\rangle_{\rm bound} - \langle\eta\rangle_p$ as functions of $\Delta\mu$ for different ϕ. The parameters are given by $\mu = 0$, $\hbar\Gamma_R = 10$ meV, $k_BT_L = 10$ meV, $k_BT_R = 1.2k_BT_L$, $E_0 = [15 + 15\sin(\Omega t + \phi)]$ meV, $\hbar\Gamma_L = [20 + 10\sin(\Omega t)]$ meV, $\Omega = 2\pi/\mathcal{T}$, and $\mathcal{T} = 10^{-11}$ s.

which specifies the general expression of the entropy production (10) in nonequilibrium quantum systems.

The thermal machine can be operated as a heat engine when the electric power $\langle W_{\rm out}\rangle > 0$. If the input energy is negative, i.e., $\langle W_I\rangle < 0$, the free energy efficiency of the heat engine is specified as [94,99–101]

$$\langle\eta\rangle_p = \frac{\langle W_{\rm out}\rangle}{(1 - T_L/T_R)\langle Q_R\rangle}, \tag{28}$$

which is consistent with the energy efficiency of steady-state thermoelectric transport [102,103], while if the input energy becomes positive, i.e., $W_I > 0$, the free energy efficiency of the heat engine is obtained as [70]

$$\langle\eta\rangle_p = \frac{\langle W_{\rm out}\rangle}{(1 - T_L/T_R)\langle Q_R\rangle + \langle W_I\rangle}. \tag{29}$$

According to the thermodynamic second law, the thermoelectric engine efficiency should have an upper bound, i.e., $\langle\eta\rangle_p \leqslant 1$ [85]. However, we note that the inclusion of the geometric effect can refine this bound.

We now demonstrate the geometric bound on efficiency in Eqs. (15) and (17). As shown in Figs. 5(a) and 6(a), we respectively illustrate the effect of the voltage bias $\Delta\mu$ and driving frequency Ω on the electric work $\langle W_{\rm out}\rangle$ per driving period. Similarly, we also show $\langle\eta\rangle_p$ in Figs. 5(b) and 6(b). Obviously, the geometric phase yields significant improvement of the maximum efficiency and output work. From the efficiency behavior of Fig. 5(b), it is found that the efficiency η_p exhibits the nonmonotonic behavior by tuning $\Delta\mu$, which is analogous with $\langle W_{\rm out}\rangle$, due to their intimate relationship as shown in Eqs. (28) and (29). Moreover, in Figs. 5(c)–5(d) and Figs. 6(c)–6(d) we plot efficiency bound $\eta_{\rm bound}$ and the

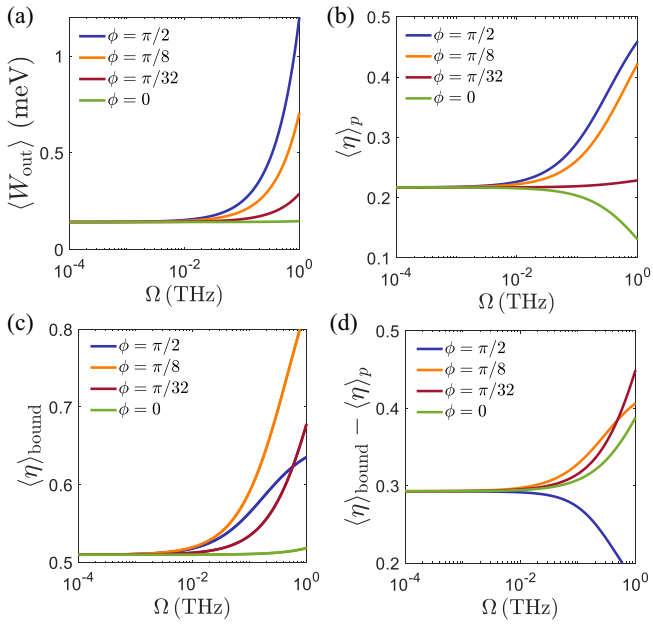

FIG. 6. (a) The output electric work $\langle W_{\rm out}\rangle$, (b) the energy efficiency $\langle\eta\rangle_p$, (c) $\langle\eta\rangle_{\rm bound}$, and (d) $\langle\eta\rangle_{\rm bound} - \langle\eta\rangle_p$ as functions of driving frequency Ω for different modulation phases. The parameters are given by $\Delta\mu = 1$ meV, $\mu = 0$, $\hbar\Gamma_R = 10$ meV, $k_BT_L = 10$ meV and $k_BT_R = 12$ meV, $E_0 = [15 + 15\sin(\Omega t + \phi)]$ meV, $\hbar\Gamma_L = [20 + 10\sin(\Omega t)]$ meV, and $\Omega = 2\pi/\mathcal{T}$.

difference $\eta_{\rm bound} - \langle\eta\rangle_p$ as functions of voltage bias $\Delta\mu$ and driving frequency Ω for a thermoelectric engine, respectively. In the parameter regime of the heat engine, the energy efficiency $\langle\eta\rangle_p$ never breaks through the boundary $\eta_{\rm bound}$. And these simulations confirm the validity of the geometric bounds. Interestingly, as shown in Figs. 5(d) and 6(d), the efficiency comes even closer to its bound, i.e., $\eta_{\rm bound} - \langle\eta\rangle_p$ approaching zero, if we optimize the geometric effect via increasing either the driving frequency or modulation phase.

Finally, we discuss the thermodynamic bounds of ϵ_p and the efficiency $\langle\eta\rangle_p$ in driven systems, compared to the steady-state ones. ϵ_p (11) is always greater than the lower bound $\epsilon_{\rm bound} \equiv 2/[1 + \langle W_{\rm out}\rangle|_{\rm geo}/\langle W_{\rm out}\rangle|_{\rm dyn}]^2$. Hence, once the geometric-phase-induced output work emerges, i.e., $\langle W_{\rm out}\rangle|_{\rm geo} \neq 0$, the lower limit of ϵ_p is generally unequal to the static counterpart 2, which is also exhibited in Fig. 3(c). Interestingly, as the geometric component exceeds the dynamic one, the lower bound may even approach 0, e.g., $\phi = \pi/8$. Such picture can be alternatively explained that though the output work is strongly enhanced by the geometric effect [Fig. 6(a)], the entropy production is not significantly increased [Fig. 3(d)]. Similarly, $\langle\eta\rangle_{\rm bound} - \langle\eta\rangle_p \geqslant 0$ is always satisfied, with the upper bound $\langle\eta\rangle_{\rm bound}$ given in Eq. (15) and Eq. (17) for $\langle W_I\rangle > 0$ and $\langle W_I\rangle < 0$, respectively, which is also illustrated in Figs. 5(d) and 6(d). Furthermore, in the positive input energy generation regime, as the geometric-phase-induced work dominates the output work, i.e., $\langle W_{\rm out}\rangle|_{\rm geo} \gg \langle W_{\rm out}\rangle|_{\rm dyn}$, the entropy production $\langle\Sigma\rangle$ is comparatively negligible to $\langle W_{\rm out}\rangle|_{\rm geo}/(k_BT_L)$, which results in the upper bound approaching the unity, while for the case of negative input energy, the efficiency bound can also reach the unity by further considering $\langle W_I\rangle \ll \langle W_{\rm out}\rangle|_{\rm geo}$. Hence, this shows the significance of the geometric phase in bounding the efficiency of heat engines by observing the fluctuation of output work. Moreover, such results are in agreement with comparable counterparts in the stochastic clock [42]. Therefore, we conclude that the geometric part of the contribution is incredible to dramatically modify the TUR.

IV. CONCLUSIONS AND PERSPECTIVES

In summary, for periodically driven systems, we have proposed a class of inequalities, termed the geometric TUR bounds, which relate the entropy production with the mean of current and its variance by bringing to light the Berry-phase-like effect. This leads to general trade-off relations among the output work, effective efficiency, entropy production, and external control protocols. The corresponding bounds indicate that the geometric phase plays a key role in constraining the relative fluctuation of currents. Moreover, such bounds provide insight into the understanding of the precision of thermoelectric heat engine. We note that our theory is able to be applied to systems arbitrarily far from equilibrium, and does not assume any specific symmetry of the system. To demonstrate the practical applicability of our results, we work out the example of a two-terminal single-level QD system, which lies within the family of thermoelectric heat engines. Our work paves the way for TUR from the geometric origin and optimizing more complex periodically driven thermoelectric heat engines.

Finally, it should be pointed out that our study is based on the Markovian approximation. The generalization of the geometric TUR in periodically driven systems to setups with non-Markovianity and quantum coherence is intriguing in future study.

ACKNOWLEDGMENTS

J.L., Z.W., J.P., and J.R. acknowledge the support by the National Natural Science Foundation of China (Grants No. 11935010 and No. 11775159) and the Natural Science Foundation of Shanghai (Grants No. 18ZR1442800 and No. 18JC1410900). C.W. acknowledges support from the National Natural Science Foundation of China (Grant No. 11704093) and the Opening Project of Shanghai Key Laboratory of Special Artificial Microstructure Materials and Technology. J.-H.J. acknowledges support from the Natural Science Foundation of China (NSFC) (Grants No. 12074281, No. 12047541, and No. 12074279), the Major Program of Natural Science Research of Jiangsu Higher Education Institutions (Grant No. 18KJA140003), the Jiangsu specially appointed professor funding, and the Academic Program Development of Jiangsu Higher Education (PAPD). J.L. also acknowledges support from the China Postdoctoral Science Foundation (Grant No. 2020M681376).

[1] P. Jung, Periodically driven stochastic systems, Phys. Rep. **234**, 175 (1993).

[2] M. Esposito, U. Harbola, and S. Mukamel, Nonequilibrium fluctuations, fluctuation theorems, and counting statistics in quantum systems, Rev. Mod. Phys. **81**, 1665 (2009).

[3] M. Campisi, P. Hänggi, and P. Talkner, Colloquium: Quantum fluctuation relations: Foundations and applications, Rev. Mod. Phys. **83**, 771 (2011).

[4] U. Seifert, Stochastic thermodynamics, fluctuation theorems and molecular machines, Rep. Prog. Phys. **75**, 126001 (2012).

[5] J. P. Pekola and B. Karimi, Colloquium: Quantum heat transport in condensed matter systems, Rev. Mod. Phys. **93**, 041001 (2021).

[6] J.-H. Jiang and Y. Imry, Linear and nonlinear mesoscopic thermoelectric transport with coupling with heat baths, C. R. Phys. **17**, 1047 (2016).

[7] G. Benenti, G. Casati, K. Saito, and R. S. Whitney, Fundamental aspects of steady-state conversion of heat to work at the nanoscale, Phys. Rep. **694**, 1 (2017).

[8] R. Wang, C. Wang, J. Lu, and J.-H. Jiang, Inelastic thermoelectric transport and fluctuations in mesoscopic system, arXiv:2112.09273.

[9] A. C. Barato and U. Seifert, Thermodynamic Uncertainty Relation for Biomolecular Processes, Phys. Rev. Lett. **114**, 158101 (2015).

[10] Y. Hasegawa, Thermodynamic Uncertainty Relation for General Open Quantum Systems, Phys. Rev. Lett. **126**, 010602 (2021).

[11] J. Liu and D. Segal, Thermodynamic uncertainty relation in quantum thermoelectric junctions, Phys. Rev. E **99**, 062141 (2019).

[12] A. M. Timpanaro, G. Guarnieri, J. Goold, and G. T. Landi, Thermodynamic Uncertainty Relations from Exchange Fluctuation Theorems, Phys. Rev. Lett. **123**, 090604 (2019).

[13] P. Pietzonka and U. Seifert, Universal Trade-Off between Power, Efficiency, and Constancy in Steady-State Heat Engines, Phys. Rev. Lett. **120**, 190602 (2018).

[14] J. M. Horowitz and T. R. Gingrich, Thermodynamic uncertainty relations constrain non-equilibrium fluctuations, Nat. Phys. **16**, 599 (2020).

[15] G. Falasco, M. Esposito, and J.-C. Delvenne, Unifying thermodynamic uncertainty relations, New J. Phys. **22**, 053046 (2020).

[16] A. Dechant and S.-i. Sasa, Fluctuation–response inequality out of equilibrium, Proc. Natl. Acad. Sci. U.S.A. **117**, 6430 (2020).

[17] K. Liu, Z. Gong, and M. Ueda, Thermodynamic Uncertainty Relation for Arbitrary Initial States, Phys. Rev. Lett. **125**, 140602 (2020).

[18] H. M. Friedman, B. K. Agarwalla, O. Shein-Lumbroso, O. Tal, and D. Segal, Thermodynamic uncertainty relation in atomic-scale quantum conductors, Phys. Rev. B **101**, 195423 (2020).

[19] Y. Hasegawa, Quantum Thermodynamic Uncertainty Relation for Continuous Measurement, Phys. Rev. Lett. **125**, 050601 (2020).

[20] S. Pal, S. Saryal, D. Segal, T. S. Mahesh, and B. K. Agarwalla, Experimental study of the thermodynamic uncertainty relation, Phys. Rev. Research **2**, 022044(R) (2020).

[21] D. Hartich and A. Godec, Thermodynamic Uncertainty Relation Bounds the Extent of Anomalous Diffusion, Phys. Rev. Lett. **127**, 080601 (2021).

[22] Y. Hasegawa, Irreversibility, Loschmidt Echo, and Thermodynamic Uncertainty Relation, Phys. Rev. Lett. **127**, 240602 (2021).

[23] J. Liu and D. Segal, Coherences and the thermodynamic uncertainty relation: Insights from quantum absorption refrigerators, Phys. Rev. E **103**, 032138 (2021).

[24] T. R. Gingrich, J. M. Horowitz, N. Perunov, and J. L. England, Dissipation Bounds All Steady-State Current Fluctuations, Phys. Rev. Lett. **116**, 120601 (2016).

[25] P. Pietzonka, F. Ritort, and U. Seifert, Finite-time generalization of the thermodynamic uncertainty relation, Phys. Rev. E **96**, 012101 (2017).

[26] K. Macieszczak, K. Brandner, and J. P. Garrahan, Unified Thermodynamic Uncertainty Relations in Linear Response, Phys. Rev. Lett. **121**, 130601 (2018).

[27] K. Proesmans and J. M. Horowitz, Hysteretic thermodynamic uncertainty relation for systems with broken time-reversal symmetry, J. Stat. Mech. (2019) 054005.

[28] S. Saryal, M. Gerry, I. Khait, D. Segal, and B. K. Agarwalla, Universal Bounds on Fluctuations in Continuous Thermal Machines, Phys. Rev. Lett. **127**, 190603 (2021).

[29] B. K. Agarwalla and D. Segal, Assessing the validity of the thermodynamic uncertainty relation in quantum systems, Phys. Rev. B **98**, 155438 (2018).

[30] K. Proesmans and C. Van den Broeck, Discrete-time thermodynamic uncertainty relation, Europhys. Lett. **119**, 20001 (2017).

[31] T. Koyuk and U. Seifert, Operationally Accessible Bounds on Fluctuations and Entropy Production in Periodically Driven Systems, Phys. Rev. Lett. **122**, 230601 (2019).

[32] T. Koyuk and U. Seifert, Thermodynamic Uncertainty Relation for Time-Dependent Driving, Phys. Rev. Lett. **125**, 260604 (2020).

[33] S. Saryal, S. Mohanta, and B. K. Agarwalla, Bounds on fluctuations for machines with broken time-reversal symmetry: A linear response study, Phys. Rev. E **105**, 024129 (2022).

[34] K. Brandner, M. Bauer, and U. Seifert, Universal Coherence-Induced Power Losses of Quantum Heat Engines in Linear Response, Phys. Rev. Lett. **119**, 170602 (2017).

[35] T. Van Vu and Y. Hasegawa, Thermodynamic uncertainty relations under arbitrary control protocols, Phys. Rev. Research **2**, 013060 (2020).

[36] K. Brandner, Coherent transport in periodically driven mesoscopic conductors: From scattering amplitudes to quantum thermodynamics, Z. Naturforsch. A **75**, 483 (2020).

[37] P. Chattopadhyay, A. Mitra, G. Paul, and V. Zarikas, Bound on efficiency of heat engine from uncertainty relation viewpoint, Entropy **23**, 439 (2021).

[38] S. Saryal, O. Sadekar, and B. K. Agarwalla, Thermodynamic uncertainty relation for energy transport in a transient regime: A model study, Phys. Rev. E **103**, 022141 (2021).

[39] H. J. D. Miller, M. H. Mohammady, M. Perarnau-Llobet, and G. Guarnieri, Thermodynamic Uncertainty Relation in Slowly Driven Quantum Heat Engines, Phys. Rev. Lett. **126**, 210603 (2021).

[40] E. Potanina, C. Flindt, M. Moskalets, and K. Brandner, Thermodynamic Bounds on Coherent Transport in Periodically Driven Conductors, Phys. Rev. X **11**, 021013 (2021).

[41] P. Menczel, E. Loisa, K. Brandner, and C. Flindt, Thermodynamic uncertainty relations for coherently driven open quantum systems, J. Phys. A: Math. Theor. **54**, 314002 (2021).

[42] A. C. Barato and U. Seifert, Cost and Precision of Brownian Clocks, Phys. Rev. X **6**, 041053 (2016).

[43] T. Koyuk, U. Seifert, and P. Pietzonka, A generalization of the thermodynamic uncertainty relation to periodically driven systems, J. Phys. A: Math. Theor. **52**, 02LT02 (2019).

[44] T. Sagawa and H. Hayakawa, Geometrical expression of excess entropy production, Phys. Rev. E **84**, 051110 (2011).

[45] T. Yuge, T. Sagawa, A. Sugita, and H. Hayakawa, Geometrical pumping in quantum transport: Quantum master equation approach, Phys. Rev. B **86**, 235308 (2012).

[46] K. Brandner, K. Saito, and U. Seifert, Thermodynamics of Micro- and Nano-Systems Driven by Periodic Temperature Variations, Phys. Rev. X **5**, 031019 (2015).

[47] K. Brandner and K. Saito, Thermodynamic Geometry of Microscopic Heat Engines, Phys. Rev. Lett. **124**, 040602 (2020).

[48] Hisao Hayakawa, Ville M. M. Paasonen, and Ryosuke Yoshii, Geometrical quantum chemical engine, arXiv:2112.12370.

[49] Gavin E. Crooks, Measuring Thermodynamic Length, Phys. Rev. Lett. **99**, 100602 (2007).

[50] P. W. Brouwer, Scattering approach to parametric pumping, Phys. Rev. B **58**, R10135 (1998).

[51] N. A. Sinitsyn and I. Nemenman, Universal Geometric Theory of Mesoscopic Stochastic Pumps and Reversible Ratchets, Phys. Rev. Lett. **99**, 220408 (2007).

[52] N. A. Sinitsyn and I. Nemenman, The Berry phase and the pump flux in stochastic chemical kinetics, Europhys. Lett. **77**, 58001 (2007).

[53] J. Ren, P. Hänggi, and B. Li, Berry-Phase-Induced Heat Pumping and Its Impact on the Fluctuation Theorem, Phys. Rev. Lett. **104**, 170601 (2010).

[54] T. Chen, X.-B. Wang, and J. Ren, Dynamic control of quantum geometric heat flux in a nonequilibrium spin-boson model, Phys. Rev. B **87**, 144303 (2013).

[55] K. L. Watanabe and H. Hayakawa, Geometric fluctuation theorem for a spin-boson system, Phys. Rev. E **96**, 022118 (2017).

[56] Y. Hino and H. Hayakawa, Fluctuation relations for adiabatic pumping, Phys. Rev. E **102**, 012115 (2020).

[57] O. Raz, Y. Subaşı, and R. Pugatch, Geometric Heat Engines Featuring Power that Grows with Efficiency, Phys. Rev. Lett. **116**, 160601 (2016).

[58] H. J. D. Miller and M. Mehboudi, Geometry of Work Fluctuations versus Efficiency in Microscopic Thermal Machines, Phys. Rev. Lett. **125**, 260602 (2020).

[59] K. Takahashi, K. Fujii, Y. Hino, and H. Hayakawa, Nonadiabatic Control of Geometric Pumping, Phys. Rev. Lett. **124**, 150602 (2020).

[60] K. Takahashi, Y. Hino, K. Fujii, and H. Hayakawa, Full counting statistics and fluctuation–dissipation relation for periodically driven two-state systems, J. Stat. Phys. **181**, 2206 (2020).

[61] Z. Wang, L. Wang, J. Chen, C. Wang, and J. Ren, Geometric heat pump: Controlling thermal transport with time-dependent modulations, Front. Phys. **17**, 1 (2022).

[62] Z. Wang, J. Chen, Z. Liu, and J. Ren, Observation of geometric heat pump effect in periodic driven thermal diffusion, arXiv:2110.10001.

[63] G. Manzano, R. Sánchez, R. Silva, G. Haack, J. B. Brask, N. Brunner, and P. P. Potts, Hybrid thermal machines: Generalized thermodynamic resources for multitasking, Phys. Rev. Research **2**, 043302 (2020).

[64] L. S. Levitov and G. B. Lesovik, Charge-transport statistics in quantum conductors, JETP Lett. **55**, 534 (1992).

[65] L. S. Levitov, H. Lee, and G. B. Lesovik, Electron counting statistics and coherent states of electric current, J. Math. Phys. **37**, 4845 (1996).

[66] J. Ren, S. Liu, and B. Li, Geometric Heat Flux for Classical Thermal Transport in Interacting Open Systems, Phys. Rev. Lett. **108**, 210603 (2012).

[67] M. V. Berry, Quantal phase factors accompanying adiabatic changes, Proc. R. Soc. London A **392**, 45 (1984).

[68] A. Bohm, A. Mostafazadeh, H. Koizumi, Q. Niu, and J. Zwanziger, *The Geometric Phase in Quantum Systems* (Springer-Verlag, New York, 2003).

[69] C. Wang, J. Ren, and J. Cao, Unifying quantum heat transfer in a nonequilibrium spin-boson model with full counting statistics, Phys. Rev. A **95**, 023610 (2017).

[70] Y. Hino and H. Hayakawa, Geometrical formulation of adiabatic pumping as a heat engine, Phys. Rev. Research **3**, 013187 (2021).

[71] Y. Izumida, Hierarchical Onsager symmetries in adiabatically driven linear irreversible heat engines, Phys. Rev. E **103**, L050101 (2021).

[72] J.-H. Jiang, Thermodynamic bounds and general properties of optimal efficiency and power in linear responses, Phys. Rev. E **90**, 042126 (2014).

[73] J.-H. Jiang, B. K. Agarwalla, and D. Segal, Efficiency Statistics and Bounds for Systems with Broken Time-Reversal Symmetry, Phys. Rev. Lett. **115**, 040601 (2015).

[74] V. Holubec and A. Ryabov, Cycling Tames Power Fluctuations near Optimum Efficiency, Phys. Rev. Lett. **121**, 120601 (2018).

[75] Crispin Gardiner and Peter Zoller, *Quantum Noise: A Handbook of Markovian and Non-Markovian Quantum Stochastic Methods with Applications to Quantum Optics* (Springer Berlin, Heidelberg, 2004).

[76] D. Segal, Heat flow in nonlinear molecular junctions: Master equation analysis, Phys. Rev. B **73**, 205415 (2006).

[77] B. K. Agarwalla, J.-H. Jiang, and D. Segal, Full counting statistics of vibrationally assisted electronic conduction: Transport and fluctuations of thermoelectric efficiency, Phys. Rev. B **92**, 245418 (2015).

[78] B. K. Agarwalla, J.-H. Jiang, and D. Segal, Quantum efficiency bound for continuous heat engines coupled to noncanonical reservoirs, Phys. Rev. B **96**, 104304 (2017).

[79] D. Segal, Stochastic Pumping of Heat: Approaching the Carnot Efficiency, Phys. Rev. Lett. **101**, 260601 (2008).

[80] J.-H. Jiang, O. Entin-Wohlman, and Y. Imry, Thermoelectric three-terminal hopping transport through one-dimensional nanosystems, Phys. Rev. B **85**, 075412 (2012).

[81] J.-H. Jiang, M. Kulkarni, D. Segal, and Y. Imry, Phonon thermoelectric transistors and rectifiers, Phys. Rev. B **92**, 045309 (2015).

[82] J. Lu, R. Wang, C. Wang, and J.-H. Jiang, Brownian thermal transistors and refrigerators in mesoscopic systems, Phys. Rev. B **102**, 125405 (2020).

[83] J. Lu, J.-H. Jiang, and Y. Imry, Unconventional four-terminal thermoelectric transport due to inelastic transport: Cooling by transverse heat current, transverse thermoelectric effect, and Maxwell demon, Phys. Rev. B **103**, 085429 (2021).

[84] G. Chen, *Nanoscale Energy Transport and Conversion* (Oxford University Press, London, 2005).

[85] H. Haug and A. P. Jauho, *Quantum Kinetics in Transport and Optics of Semiconductors* (Springer-Verlag, Berlin, 2008).

[86] J. Lu, R. Wang, J. Ren, M. Kulkarni, and J.-H. Jiang, Quantum-dot circuit-QED thermoelectric diodes and transistors, Phys. Rev. B **99**, 035129 (2019).

[87] M. F. Ludovico, L. Arrachea, M. Moskalets, and D. Sánchez, Probing the energy reactance with adiabatically driven quantum dots, Phys. Rev. B **97**, 041416(R) (2018).

[88] G. Li, B.-Z. Hu, N. Yang, and J.-T. Lü, Temperature-dependent thermal transport of single molecular junctions from semiclassical Langevin molecular dynamics, Phys. Rev. B **104**, 245413 (2021).

[89] A. Solfanelli, M. Falsetti, and M. Campisi, Nonadiabatic single-qubit quantum Otto engine, Phys. Rev. B **101**, 054513 (2020).

[90] L. M. Cangemi, M. Carrega, A. De Candia, V. Cataudella, G. De Filippis, M. Sassetti, and G. Benenti, Optimal energy conversion through antiadiabatic driving breaking time-reversal symmetry, Phys. Rev. Research **3**, 013237 (2021).

[91] N. Piccione, G. De Chiara, and B. Bellomo, Power maximization of two-stroke quantum thermal machines, Phys. Rev. A **103**, 032211 (2021).

[92] B. Bhandari, P. T. Alonso, F. Taddei, F. von Oppen, R. Fazio, and L. Arrachea, Geometric properties of adiabatic quantum thermal machines, Phys. Rev. B **102**, 155407 (2020).

[93] J. Liu, K. A. Jung, and D. Segal, Periodically Driven Quantum Thermal Machines from Warming up to Limit Cycle, Phys. Rev. Lett. **127**, 200602 (2021).

[94] P. T. Alonso, P. Abiuso, M. Perarnau-Llobet, and L. Arrachea, Geometric optimization of non-equilibrium adiabatic thermal machines and implementation in a qubit system, arXiv:2109.12648.

[95] G. Jaliel, R. K. Puddy, R. Sánchez, A. N. Jordan, B. Sothmann, I. Farrer, J. P. Griffiths, D. A. Ritchie, and C. G. Smith, Experimental Realization of a Quantum Dot Energy Harvester, Phys. Rev. Lett. **123**, 117701 (2019).

[96] O. Maillet, P. A. Erdman, V. Cavina, B. Bhandari, E. T. Mannila, J. T. Peltonen, A. Mari, F. Taddei, C. Jarzynski, V. Giovannetti, and J. P. Pekola, Optimal Probabilistic Work Extraction beyond the Free Energy Difference with a Single-Electron Device, Phys. Rev. Lett. **122**, 150604 (2019).

[97] M. Josefsson, A. Svilans, A. M. Burke, E. A. Hoffmann, S. Fahlvik, C. Thelander, M. Leijnse, and H. Linke, A quantum-dot heat engine operating close to the thermodynamic efficiency limits, Nat. Nanotechnol. **13**, 920 (2018).

[98] M. F. Ludovico, L. Arrachea, M. Moskalets, and D. Sanchez, Periodic energy transport and entropy production in quantum electronics, Entropy **18**, 419 (2016).

[99] J.-H. Jiang, Enhancing efficiency and power of quantum-dots resonant tunneling thermoelectrics in three-terminal geometry by cooperative effects, J. Appl. Phys. **116**, 194303 (2014).

[100] M. F. Ludovico, M. Moskalets, D. Sánchez, and L. Arrachea, Dynamics of energy transport and entropy production in ac-driven quantum electron systems, Phys. Rev. B **94**, 035436 (2016).

[101] M. F. Ludovico, F. Battista, F. von Oppen, and L. Arrachea, Adiabatic response and quantum thermoelectrics for ac-driven quantum systems, Phys. Rev. B **93**, 075136 (2016).

[102] J. Lu, R. Wang, Y. Liu, and J.-H. Jiang, Thermoelectric cooperative effect in three-terminal elastic transport through a quantum dot, J. Appl. Phys. **122**, 044301 (2017).

[103] J.-H. Jiang and Y. Imry, Enhancing Thermoelectric Performance Using Nonlinear Transport Effects, Phys. Rev. Appl. **7**, 064001 (2017).